Journal of Thermal Analysis and Calorimetry (2019) 137:1225–1232
https://doi.org/10.1007/s10973-019-08041-x

Form-stable phase change materials based on castor oil and palmitic acid for renewable thermal energy storage

Bo Wu[1] · Yuanyang Zhao[1] · Qinfeng Liu[1] · Changlin Zhou[1] · Xi Zhang[1] · Jingxin Lei[1]

Received: 10 August 2018 / Accepted: 24 January 2019 / Published online: 31 January 2019

Abstract
Utilization of renewable biomass to prepare phase change material (PCM) that can reversibly store renewable thermal energy is of great interest. Castor oil with functional hydroxyl groups is especially attractive for the preparation of polymeric materials. In this work, a novel castor oil-based polyurethane-acrylate oligomer (COPUA) was firstly synthesized through a two-step condensation reaction. Followed by in situ polymerization of COPUA in the presence of palmitic acid (PA), a novel biomass-based form-stable PCM was prepared, in which renewable PA serves as phase change functional ingredient and castor oil-based crosslinking network acts as encapsulation material. Tailoring the mass ratio of PA and COPUA provides the ultimate encapsulation ratio (70%) of PA in form-stable PCM. The chemical structure, crystalline property, thermal property of form-stable PCM were characterized using Fourier transform infrared spectroscopy, wide-angle X-ray diffraction, differential scanning calorimetry and thermogravimetric. Those results demonstrate that the prepared form-stable PCM possesses that good thermal storage capacity with the phase change enthalpy reaches 141.2 J g^{-1}. Accelerated thermal cycling test was also performed to illustrate the thermal reliability of form-stable PCM.

Keywords Castor oil · Phase change materials · Palmitic acid · Renewable biomass · Thermal energy storage

Introduction

The large-scale utilizations of petroleum-based energy have caused many environmental concerns. To address those problems, focus is on the utilization of renewable energy (e.g., solar energy and geothermal energy) [1–3]. However, those energy supplies often change over time, enlarging the mismatch between supply and demand. Thermal energy storage (TES) can effectively be used to improve the performance and reliability of those energy supplies [4]. Further, phase change materials (PCMs) featuring low-cost and nontoxic composition have been proved to be one of the economical, feasible and eco-friendly technologies for TES [5–7]. They function by releasing energy during the crystallization process with the formation of crystals. This energy storage strategy can be applied in various areas. For instance, building materials equipped with PCMs are capable of reducing temperature variations during day and night, which effectively reduce the electrical energy consumption by air condition system [8–10].

There are mainly two types of encapsulation materials for form-stable PCMs: One is inorganic encapsulation materials, and another is polymeric encapsulation materials. Inorganic materials including expanded graphite [11], diatomite [12], montmorillonite [13], perlite [10], vermiculite [14] offer advantages of high thermal stability, low cost and inertness. It has been accepted that the encapsulation forces of inorganic encapsulation materials are based on the capillary and surface tension of porous structures [10–14]. However, the encapsulation rates, which directly determine thermal storage capacity, are severely restricted due to the limit porous structures. For instance, diatomite was successively dealt with high-temperature calcination, acid treatment and alkali leaching before encapsulation, and the maximum load of PEG only increases from 32 to 63 mass% [12]. Compared with inorganic encapsulation materials, polymeric encapsulation materials offer some

✉ Jingxin Lei
jxlei@scu.edu.cn

[1] State Key Laboratory of Polymer Materials Engineering, Polymer Research Institute of Sichuan University, Chengdu 610065, China

merits. Firstly, they are commonly synthesized with various synthesis routes which can be designed and tuned to meet specific dimension, offering a wide structural diversity [15–18]. Second, the encapsulation rate is much higher than inorganic encapsulation materials due to their outstanding frame and restriction effect [19]. Third, a large number of polymeric encapsulation materials can be directly obtained from natural renewable resource or prepared from their derivatives [20–23]. In general, the widespread utilizations of petroleum-based and nonrenewable polymeric materials have also raised many environmental concerns and resource shortage problems. The demand for polymeric materials prepared from natural, renewable and biodegradable materials is increasing, as the demand for renewable energy. Hence, exploring polymeric encapsulation material derived from sustainable biomass with low cost and high abundance is of great prospects. Many readily available, renewable biomasses such as starches, celluloses, proteins and vegetable oils have been developed to synthesis polymeric materials [24–26]. Till date many renewable biomasses have been reported for the preparation of form-stable PCMs [20–23]. For example, Şentürk et al. [20] prepared three kinds of PEG-based form-stable PCMs using cellulose, agarose and chitosan as encapsulation materials. Chen et al. [23] studied the morphology and thermal properties of PEG/cellulose acetate composite ultrafine fibers as new form-stable PCMs for TES. Ma et al. [27] developed a form-stable PCMs based on wood flour and a eutectic mixture of lauric acid and myristic acid using a vacuum impregnation method. Many other biomasses also have great potential in the preparation of form-stable PCMs for TES [21, 22].

Castor oils, mainly consisting of ricinoleic acid (12-hydroxy-cis-9-octadecenoic acid), are obtained from extracting or expressing the seeds of Ricinus communis. Compared with other vegetable oils, castor oils (CO) possess hydroxyl groups, which can be utilized directly to prepare polymeric materials without modification [28–30]. In our previous studies, castor oil was adopted as crosslinking agent to prepare crosslinked polyurethane solid–solid PCMs, while PEG was used as phase change ingredient [31]. However, it has associated problems such as complex preparation condition and severe restriction of PEG chain movement causing loss of phase change enthalpy. As we know, palmitic acid (PA) is one of the most widely available, biodegradable and eco-friendly fatty acids [32–34]. In this work, a multifunctional CO-based polyurethane-acrylate oligomer (COPUA) was synthesized through the reaction between CO, isophorone diisocyanate (IPDI) and hydroxyethyl methylacrylate (HMEA). So double bonds were chemically bonded to CO. Next, form-stable PCMs were prepared by blending COPUA with PA followed by in situ polymerization using 2,2-azobisisobutyronitrile (AIBN) as initiator. The polymerized COPUA functions as encapsulation material, and the encapsulated PA acted as phase change intergradient. To our knowledge, COPUA was the first time to be used for the preparation of form-stable PCMs, which is environmentally benign and sustainable. Chemical structure and crystalline property of the prepared form-stable PCMs were confirmed by Fourier transform infrared spectroscopy (FTIR) and wide-angle X-ray diffraction (WXRD), respectively. Thermal properties including thermal storage capacity and thermal stability were, respectively, studied using differential scanning calorimetry (DSC) and thermogravimetric (TG). Accelerated thermal cycling test was also adopted to investigate the thermal reliability and reusability of form-stable PCMs. This design of CO is of particular interest as it can enlarge the application of renewable CO, especially for the storage of renewable thermal energy.

Experimental

Materials

Castor oil (CO, analytical grade, hydroxyl number equals 163 mg KOH/g) and hydroxyethyl methylacrylate (HMEA, analytical grade, 99% purity) purchased from Chengdu Kelong Chemical Reagent Co. Ltd. (China) were dried under vacuum condition at 110 °C for 4 h prior to use. Isophorone diisocyanate (IPDI, analytical grade, 98% purity) was supplied by Aladdin chemistry regent Co., Ltd. (China), used as received. 2,2-Azobisisobutyronitrile (AIBN, analytical grade, 98% purity), dibutyltin dilaurate (DBTDL, analytical grade, 98% purity) and palmitic acid (PA, analytical grade, 98% purity) were also obtained from Chengdu Kelong Chemical Reagent Co. Ltd. (China).

Synthesis of COPUA

COPUA was synthesized in two steps, and the corresponding synthesis route is shown in Scheme 1. In the first step 22.2 g (100 mmol) IPDI and a drop of DBTDL were placed in a three-neck-round-bottom flask fitted with an overhead stirrer, nitrogen inlet and an addition funnel and then dropwise added 13 g (100 mmol) HMEA at 20 °C. The mixture was kept and stirred at 20 °C until the isocyanate reached the theoretical value which was determined by chemical titration. In the second step, 34 g (containing 100 mmol hydroxy) CO was dropwise added into the aforementioned mixture. The reaction mixture was continuously stirred at 20 °C for 24 h and 60 °C for 12 h until the absorption peak of the –NCO group in the FTIR disappeared.

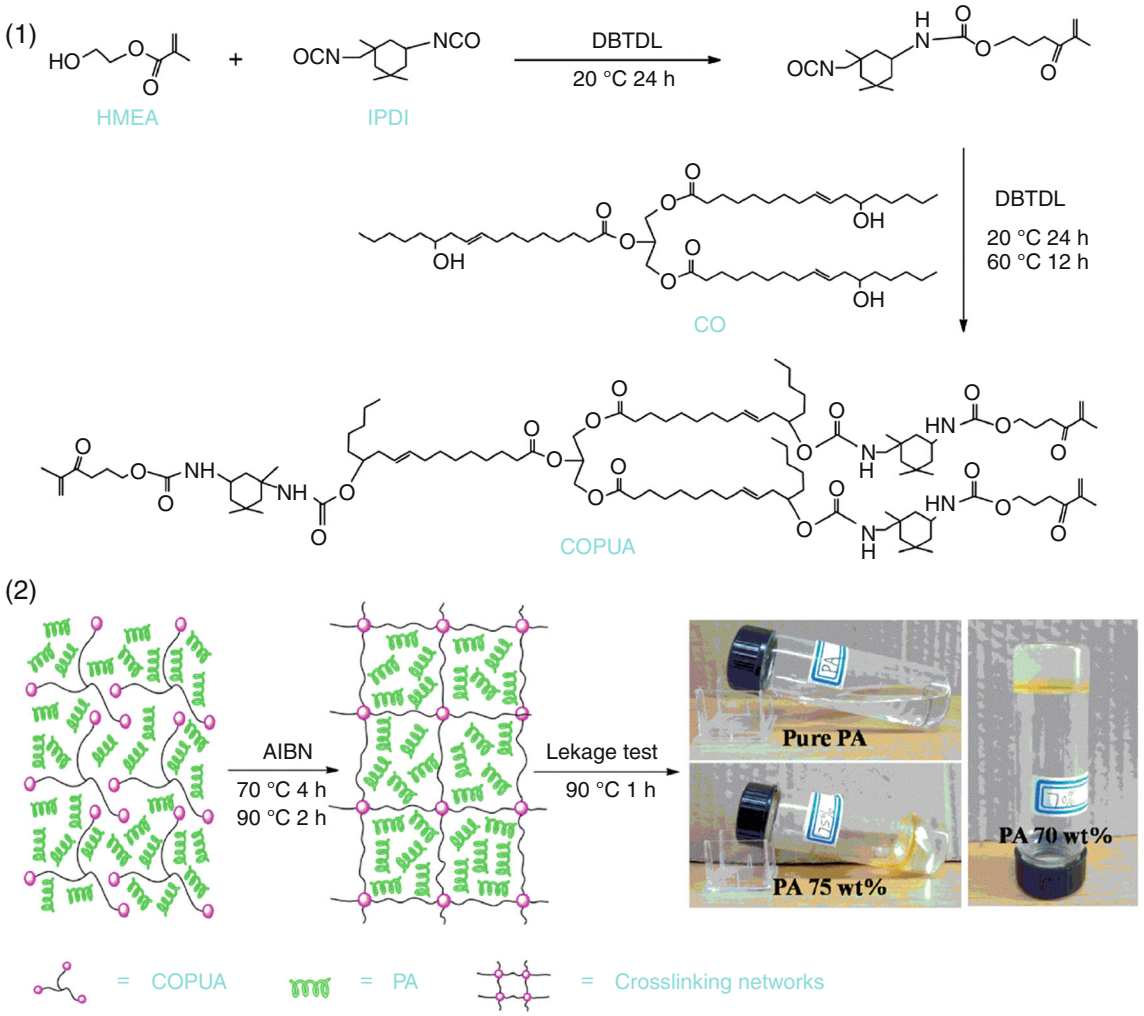

Scheme 1 Schematic synthesis route of COPUA and form-stable PCM

Preparation of form-stable PCM

Form-stable PCMs were prepared by using the in situ polymerization method. In a typical preparation process, the predetermined PA and COPUA were poured into a 100-mL round-bottom flask, followed by heating the flask at 70 °C until the homogeneous mixing of PA and COPUA. Next, a certain amount of AIBN (1 mass% of the total mass of PA and COPUA) was added into the aforementioned mixture, and the mixture was quickly stirred for homogenization. After homogenization, the reaction mixture was transferred to a vacuum oven for achieving completely curing. The curing procedure was performed under nitrogen atmosphere at 70 °C for 2 h and 90 °C for 2 h. To determine the maximum encapsulation rate, a series of PA/crosslinked COPUA composite with different PA mass fractions were prepared. All the prepared composites were underwent leakage test by heating them to 90 °C (higher than their phase change temperature) for 1 h. The composite displaying no liquid leakage during the whole heating process was determined as form-stable PCMs. The linkage test results show that pure PA turns into transparent liquid totally when the temperature remains at 90 °C. It is clear in Scheme 1 that there is no liquid appeared when PA mass fraction is 70 mass%; however, the liquid can be observed when PA mass fraction reaches 75 mass%. Those results suggest that the maximum encapsulation ratio of PA is 70 mass%, and the crosslinked COPUA with 70 mass% PA is confirmed as form-stable PCM. For comparison, the crosslinked COPUA without PA is termed as blank sample.

Methods

Fourier transform infrared spectroscopy (FTIR) profile was obtained using FTIR spectrometer (iS10 Thermo Nicolet Co., Ltd, Madison, America) with the scanning range from 4000 to 400 cm^{-1}. Note that the measured pattern for form

stable was attenuated total reflection. Wide-angle X-ray diffraction (WXRD) profiles were recorded using high-resolution wide-angle X-ray diffractometer (Rigaku Co., Ltd, Japan) within the scan range from 5° to 50° with a scanning rate of 2° min^{-1} at room temperature. Different scanning calorimetry (DSC) was performed on a differential scanning calorimeter (DSC 204 F1, German) at 10 °C min^{-1} rate in temperature window 0–95 °C under nitrogen atmosphere. Around 8 mg of specimen was used for each testing. To eliminate the heat history of materials, each specimen was heated from 40 to 100 °C before formal testing. Thermogravimetric analysis (TG) was performed on a SDT-Q600 thermo-analyzer instrument from 30 to 650 °C under nitrogen atmosphere with a linear heating rate of 10 °C min^{-1}. Around 8 mg of specimen was used for each testing.

To identify the thermal reliability of form-stable PCM, accelerated thermal cycling test was carried out in a high–low-temperature chamber (GDH-2010B, Shanghai Jinghong Co., Ltd). The typical procedure is as follows; around 10 g of form-stable PCM was treated with 100 and 1000 consecutive heating and cooling in the temperature range of 20–90 °C. Subsequently, it was tested by FTIR and DSC to investigate the variations of chemical and phase change characteristic.

Results and discussion

Chemical structure analysis

The chemical structure of COPUA was identified through FTIR. From Fig. 1a, the peaks at 3361 cm^{-1}, 1722 cm^{-1} and 1522 cm^{-1} are associated with N–H groups and C=O

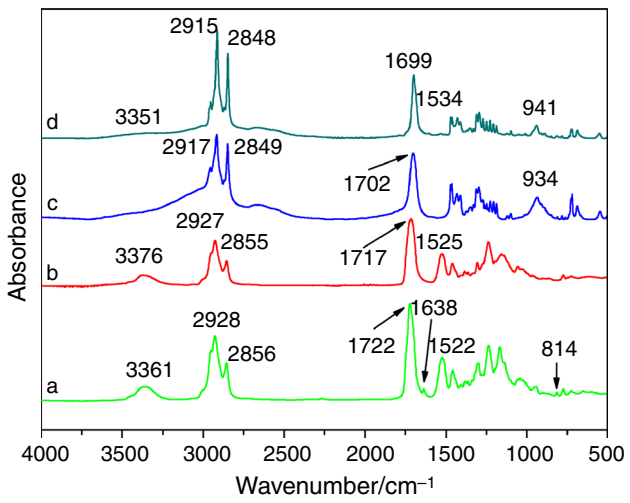

Fig. 1 FTIR profiles of **a** COPUA, **b** blank sample, **c** pure PA and **d** form-stable PCM

groups from carbamate linkages. Obvious peaks around 2928 cm^{-1} and 2856 cm^{-1} represent the asymmetrical and symmetrical stretching vibration of $–CH_2$ and $–CH_3$ groups. And the characteristic peaks at 1638 cm^{-1} and 814 cm^{-1} are resulted from the stretching and bending vibrations of the C=C–H groups and provide the evidence of successful introduction of double bonds into COPUA. From the above results, COPUA was successfully synthesized.

To confirm the chemical structure, FTIR profile of PA, blank sample and form-stable PCMs is also shown in Fig. 1. The FTIR spectrum of blank sample is shown in Fig. 1b, the characteristic peaks at 3367 cm^{-1}, 1525 cm^{-1} and 1717 cm^{-1} remain existent, while the characteristic peak at 1638 cm^{-1} and 814 cm^{-1} of C=C groups is completely disappeared, suggesting the successful polymerization of COPUA. Figure 1c presents the FTIR spectrum of pure PA in which the characteristic peaks around 2917 cm^{-1} and 2849 cm^{-1} are attributed to the asymmetrical and symmetrical stretching vibration of $–CH_2$ and $–CH_3$ groups. The obvious peak at 1702 cm^{-1} belongs to the stretching vibration of C=O groups, and the broad peak at 934 cm^{-1} is assigned to the bending vibration of –OH groups (carboxyl). It should be noted that the strong absorption peaks at 3017 cm^{-1} and 2848 cm^{-1} represent the stretching vibrations of the –COOH groups, which are covered by the stretching vibration of $–CH_2$ and $–CH_3$ groups. As shown in Fig. 1d, form-stable PCM has characteristic bands peaked at 3351 cm^{-1}, 1534 cm^{-1}, 2915 cm^{-1}, 2848 cm^{-1}, 1699 cm^{-1} and 941 cm^{-1}, which can be indexed to the vibration of N–H groups from carbamate linkages, aliphatic C–H groups from $–CH_2$ and $–CH_3$, –C=O groups and –OH groups from carboxyl and ester, respectively. Clearly, the C=C–H stretching and bending vibrations observed at around 1638 cm^{-1} and 814 cm^{-1}, respectively, in case of COPUA are absent in form-stable PCM. Further the presence of –COOH stretching vibration at around 2800–3200 cm^{-1} indicates the successful preparation of form-stable PCM. There are no any characteristic brands that are different from pure PA and blank sample, indicating the absence of reaction between PA with crosslinked COPUA. From those results, we can conclude that pure PA is physically encapsulated into crosslinking networks formed by COPUA.

Crystalline property analysis

Since the thermal capacity of PCMs is related to the phase transition of functional intergradient between crystallization state and amorphous state, crystalline properties of PCMs are significant. The XRD profile of PA, blank sample and form-stable PCMs is shown in Fig. 2. In the XRD spectra of pure PA (dot line), it displays two

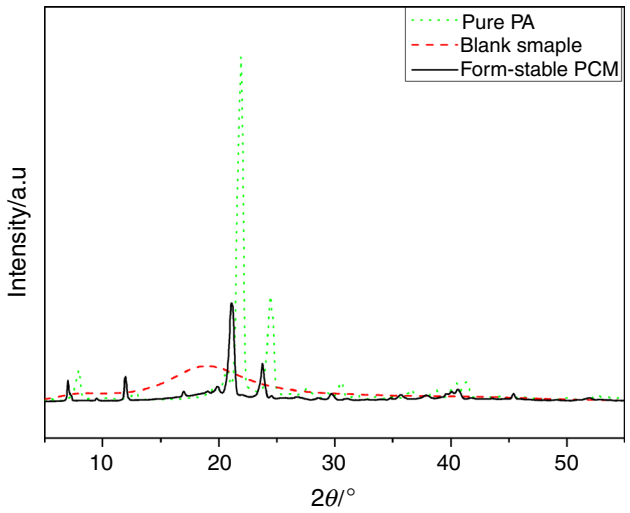

Fig. 2 WXRD profiles of pure PA, blank sample and form-stable PCM

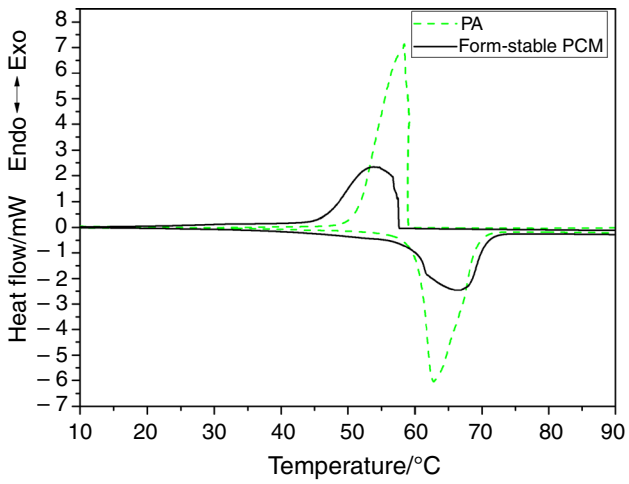

Fig. 3 DSC profiles of pure PA (dash line) and form-stable PCM (solid line)

characteristic peaks centered at 21.9° and 24.4°, which indicates the good crystalline property of pure PA. In the XRD spectra of blank sample (dash line), there is only broad and flat diffraction peak and no characteristic peak is observed because of its amorphous structure. In the XRD spectra of form-stable PCM (solid line), the similar diffraction peaks at 21.1° and 23.4° are also presented, implying that crystalline structure of form-stable PCM is similar to the pure PA and form-stable PCM also has good crystalline property. However, the diffraction peak intensities of form-stable PCM are smaller than that of pure PA and the peak position of them is slightly different. This can be explained by the fact that the crystalline capacity of PA in form-stable PCMs is seized with the constraint imposed by crosslinking networks. Actually, the crystallization of form-stable PCM is the crystallization of PA chains. As many previous literatures reported, rigid crosslinking networks in form-stable PCM restrain the free movement and orientation of PA chains, leading to the decrease in crystallinity [23, 35]. Although the presence of crosslinking networks is negative for the crystallization of PA, it plays an important role in preventing the linkage of amorphous PA.

Phase change property analysis

Phase change properties including phase change temperatures and phase change enthalpies are very important for practical thermal energy storage. The DSC profiles of pure PA and form-stable PCM are shown in Fig. 3, and the detailed results are tabulated in Table 1. As can be seen from Fig. 3, both pure PA and form-stable PCM have obvious exothermic and endothermic behaviors during heating and cooling programs, respectively, suggesting their reversible thermal storage and release capacities. In addition, the DSC curves show only one pair of exothermic/endothermic peaks and further testify the good and homogeneous crystalline properties of pure PA and form-stable PCM. As we know, the prepared form-stable PCMs function by the reversible melting and freezing of PA crystals. Thermal storage process (charging process) starts during the phase change from crystalline state to amorphous state corresponding to the endothermic peak. In contrast, the stored thermal energy will release (discharging process), while the temperature drops down to freezing temperature, which is resented by the exothermic peak. For pure PA shown in Table 1, the thermal storage occurs at 62.8 °C with the melting latent heat of 217.8 J g^{-1}; the stored thermal energy will release once the temperature is below 58.48 °C with the freezing latent heat of 220.4 J g^{-1}. Melting and freezing temperatures for form-stable PCM obtained through DSC profiles are 66.6 °C and 54.3 °C, respectively, and the melting and freezing latent heat, respectively, reach 141.2 J g^{-1} and 137.1 J g^{-1}. Those results suggest that 1 g form-stable PCM can store approximately 141.2 J thermal energy during the heating process from 55 to 70 °C and release around 137.1 J thermal energy once the temperature decreases from 60 to 45 °C. Meanwhile, it is obvious in Table 1 that the melting and freezing latent heat of form-stable PCM are lower than that of theoretical values. This phenomenon is ascribed to the imperfect crystalline property of form-stable PCM, in which the free movement and orientation of PA chains are restricted by crosslinking networks. Depending on the thermal storage mechanism, thermal storage capacity of form-stable PCM is affected by the crystallinity, which will in turn reflect the crystallinity.

Table 1 Phase change properties of pure PA and form-stable PCM from DSC diagrams

Sample	Pure PA	Form-stable PCM		
		Before thermal cycling	After 100 thermal cycles	After 1000 thermal cycles
T_m/°C	62.8	66.57	66.45	66.43
ΔH_m/J g^{-1}	217.8	141.2	139.2	114.9
T_f/°C	58.48	54.32	53.92	52.28
ΔH_f/J g^{-1}	220.4	137.1	133.8	96.3

T_m and T_f represent melting and freezing temperatures, respectively; ΔH_m and ΔH_f are the melting and freezing latent heat, respectively

Thermal stability analysis

Figure 4 shows the TG profiles and DTG profiles of pure PA, blank sample and form-stable PCM. As can be seen from Fig. 4a, pure PA shows a single thermal decomposition which starts from 194.5 °C and ends at 262.4 °C. And Fig. 4b shows that the maximum decomposition rate happens at 249.5 °C. Different from pure PA, blank sample shows two steps of thermal decomposition, namely a decomposition from 271.5 to 386 °C followed by a decomposition from 386 to 447.9 °C. Their maximum decomposition rates appear at 332.7 and 428.1 °C, respectively. The first decomposition is resulted from the degradation of urethane bonds, and the second decomposition can be ascribed to the degradation of ester bonds and carbon–carbon bonds. It is obvious in Fig. 4 that form-stable PCM displays three-step thermal decomposition, just like the combination of pure PA and blank samples. Apparently, the first decomposition corresponds to the volatilization of the PA so that the mass loss is nearly 70 mass%. The second and third decompositions of form-stable PCM are identical to the decomposition of crosslinking networks (blank sample). It can be seen from Fig. 4a that the decomposition temperature of form-stable PCM at 5 mass% mass losses is 180.4 °C. So the prepared form-stable PCM is available for solar energy storage, in which the operating temperature is usually below 80 °C.

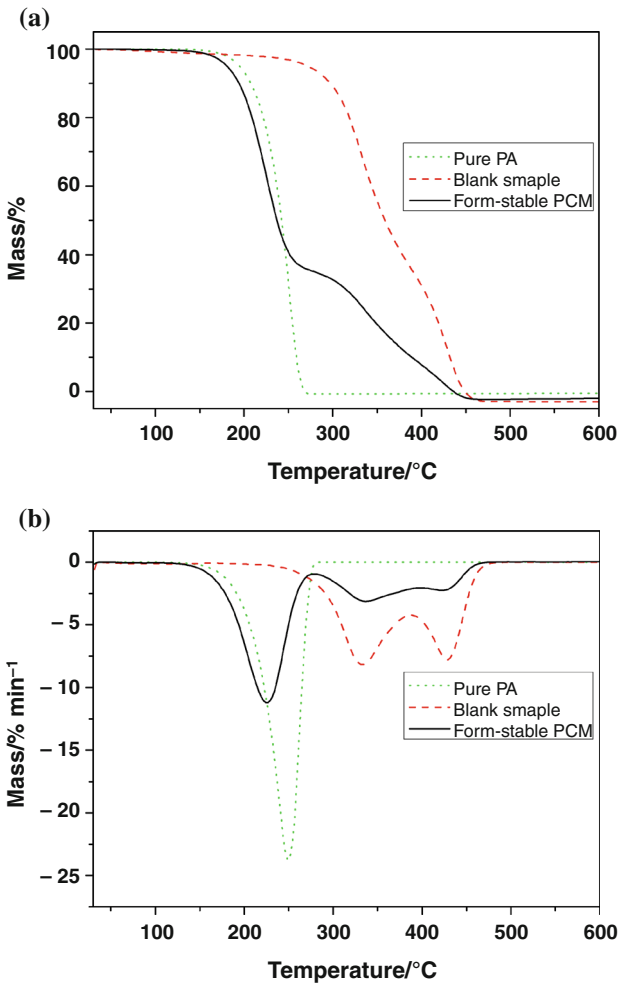

Fig. 4 Thermal stability analysis of pure PA, blank sample and form-stable PCM **a** TG and **b** DTG profiles

Thermal reliability analysis

To confirm the chemical reliability of form-stable PCM, FTIR profiles before and after 100 thermal cycles are shown in Fig. 5a. There are no different absorption bands between two FTIR profiles, indicating that the chemical structure of form-stable PCM did not change during the accelerated thermal cycling test. The prepared form-stable PCM has good reliability and durability in terms of chemical structure.

To further illustrate the reliability and durability of form-stable PCM, the DSC profiles before and after thermal cycling test are shown in Fig. 5b, and the detailed phase change characteristics are tabulated in Table 1. It is obvious in Fig. 5b that the exothermic peaks for both DSC curves at around 54 °C are due to the crystallization of PA chains, while their corresponding endothermic peaks at around 66.5 °C are ascribed to the melting of PA crystals. It can be concluded that 100 times of thermal cycling test did not change the reversible thermal storage property of form-stable PCM. As can be seen from Table 1, the

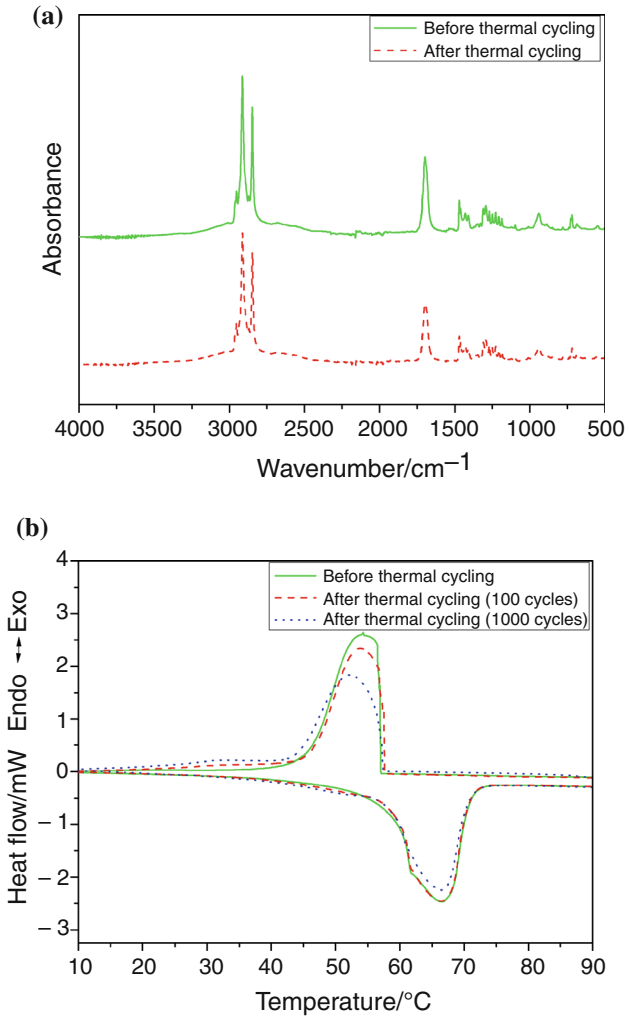

Fig. 5 Thermal reliability analysis of form-stable PCMs **a** FTIR profiles and **b** DSC profiles before thermal cycling test, after 100 thermal cycles and after 1000 thermal cycles

variations of melting and freezing latent heat are negligible after 100 thermal cycles, suggesting that the prepared form-stable PCM possesses good thermal reliability and reusability within 100 thermal cycles. This is because the crosslinking network has good thermal stability and cohesiveness as well as excellent mechanical property, which play a significant frame and restriction role to encapsulate PA and prevent melt PA from leakage. The DSC profiles of form-stable PCM after 1000 thermal cycles test are also recorded in Fig. 5b. Even after 1000 times thermal cycling test, the prepared form-stable PCMs still have a melting latent heat of 114.9 J g^{-1} and a freezing latent heat of 96.3 J g^{-1}, which is slightly decreased compared to pristine sample. The melting and freezing points of form-stable PCM after 1000 thermal cycles also show little changes. When form-stable PCM experiences a long-term sequential thermal cycling test, some chemical bonds in COPUA are partially ruptured, leading to the slight leakage of PA. As a result, the melting and freezing latent heat are decreased to some extent. Because of the existence of crosslinks in form-stable PCM, it still displays a good thermal storage capacity. Hence, the prepared form-stable PCM has excellent thermal reliability in terms of phase change characteristics and displays a good shape stable property during phase change.

Conclusions

In this work, castor oil-based form-stable PCM for renewable thermal energy storage was successfully prepared through in situ polymerization. Both the phase change functional ingredient and encapsulation materials are derived from renewable biomasses. The prepared form-stable PCM displays good shape stability at 90 °C, and the maximum encapsulation rate is 70 mass%. FTIR identifies that the chemical structure of COPUA and form-stable PCM is the same as our design. WXRD results suggest that the prepared form-stable PCM possesses similar crystalline structure as pure PA, but their crystallinity is deteriorated due to the restriction effect of crosslinking networks. DSC results show that form-stable PCM has reversible thermal storage and release capacity in the temperature range of 54.3 °C and 66.6 °C. Meanwhile, the melting and freezing latent heat of form-stable PCM reach up to 141.2 J g^{-1} and 137.1 J g^{-1}. TG results demonstrate that form-stable PCM is supposed to be applied for thermal energy storage where the operating temperature is lower than 180 °C. Accelerated thermal cycling test certifies that form-stable PCM is reliable and durable in terms of chemical structure and phase change characteristics after 100 times thermal cycles. Even after 1000 thermal cycles, the prepared form-stable PCM remains high melting and freezing latent heat. The prepared form-stable PCM has potential for solar energy storage, waste heat recovery and many other engineering areas.

References

1. McKone JR, DiSalvo FJ, Abru AHD. Solar energy conversion, storage, and release using an integrated solar-driven redox flow battery. J Mater Chem A. 2017;5:5362–72.
2. Börjesson K, Lennartson A, Moth-Poulsen K. Efficiency limit of molecular solar thermal energy collecting devices. ACS Sustain Chem Eng. 2013;1:585–90.
3. Ellabban O, Abu-Rub H, Blaabjerg F. Renewable energy resources: current status, future prospects and their enabling technology. Renew Sustain Energy Rev. 2014;39:748–64.

4. Alva G, Liu L, Huang X, Fang G. Thermal energy storage materials and systems for solar energy applications. Renew Sustain Energy Rev. 2017;68:693–706.
5. Sundararajan S, Samui AB, Kulkarni PS. Versatility of polyethylene glycol (PEG) in designing solid-solid phase change materials (PCMs) for thermal management and their application to innovative technologies. J Mater Chem A. 2017;5:18379–96.
6. Pielichowska K, Pielichowski K. Phase change materials for thermal energy storage. Prog Mater Sci. 2014;65:67–123.
7. Wu B, Fu W, Kong B, Hu K, Zhou C, Lei J. Preparation and characterization of stearic acid/polyurethane composites as dual phase change material for thermal energy storage. J Therm Anal Calorim. 2018;132:907–17.
8. Zhou D, Zhao CY, Tian Y. Review on thermal energy storage with phase change materials (PCMs) in building applications. Appl Energy. 2012;92:593–605.
9. Akeiber H, Nejat P, Majid MZA, Wahid MA, Jomehzadeh F, Zeynali Famileh I, Calautit JK, Hughes BR, Zaki SA. A review on phase change material (PCM) for sustainable passive cooling in building envelopes. Renew Sustain Energy Rev. 2016;60:1470–97.
10. Karaipekli A, Biçer A, Sarı A, Tyagi VV. Thermal characteristics of expanded perlite/paraffin composite phase change material with enhanced thermal conductivity using carbon nanotubes. Energy Convers Manag. 2017;134:373–81.
11. Zhang N, Yuan Y, Wang X, Cao X, Yang X, Hu S. Preparation and characterization of lauric–myristic–palmitic acid ternary eutectic mixtures/expanded graphite composite phase change material for thermal energy storage. Chem Eng J. 2013;231:214–9.
12. Qian T, Li J, Min X, Guan W, Deng Y, Ning L. Enhanced thermal conductivity of PEG/diatomite shape-stabilized phase change materials with Ag nanoparticles for thermal energy storage. J Mater Chem A. 2015;3:8526–36.
13. Fang X, Zhang Z, Chen Z. Study on preparation of montmorillonite-based composite phase change materials and their applications in thermal storage building materials. Energy Convers Manag. 2008;49:718–23.
14. Deng Y, Li J, Qian T, Guan W, Li Y, Yin X. Thermal conductivity enhancement of polyethylene glycol/expanded vermiculite shape-stabilized composite phase change materials with silver nanowire for thermal energy storage. Chem Eng J. 2016;295:427–35.
15. Chen Z, Wang J, Yu F, Zhang Z, Gao X. Preparation and properties of graphene oxide-modified poly(melamine-formaldehyde) microcapsules containing phase change material n-dodecanol for thermal energy storage. J Mater Chem A. 2015;3:11624–30.
16. Tang B, Wang L, Xu Y, Xiu J, Zhang S. Hexadecanol/phase change polyurethane composite as form-stable phase change material for thermal energy storage. Sol Energy Mater Sol Cells. 2016;144:1–6.
17. Lian Q, Li K, Sayyed AAS, Cheng J, Zhang J. Study on a reliable epoxy-based phase change material: facile preparation, tunable properties, and phase/microphase separation behavior. J Mater Chem A. 2017;5:14562–74.
18. Wu B, Jiang Y, Wang Y, Zhou C, Zhang X, Lei J. Study on a PEG/epoxy shape-stabilized phase change material: preparation, thermal properties and thermal storage performance. Int J Heat Mass Transf. 2018;126:1134–42.
19. Wu D, Wen W, Chen S, Zhang H. Preparation and properties of a novel form-stable phase change material based on a gelator. J Mater Chem A. 2015;3:2589–600.
20. Şentürk SB, Kahraman D, Alkan C, Gökçe İ. Biodegradable PEG/cellulose, PEG/agarose and PEG/chitosan blends as shape stabilized phase change materials for latent heat energy storage. Carbohydr Polym. 2011;84:141–4.
21. Jiang Y, Ding E, Li G. Study on transition characteristics of PEG/CDA solid–solid phase change materials. Polymer. 2002;43:117–22.
22. Kumar A, Kulkarni PS, Samui AB. Polyethylene glycol grafted cotton as phase change polymer. Cellulose. 2014;21:685–96.
23. Chen C, Wang L, Huang Y. Crosslinking of the electrospun polyethylene glycol/cellulose acetate composite fibers as shape-stabilized phase change materials. Mater Lett. 2009;63:569–71.
24. Xia Y, Larock RC. Vegetable oil-based polymeric materials: synthesis, properties, and applications. Green Chem. 2010;12:1893.
25. Fertier L, Koleilat H, Stemmelen M, Giani O, Joly-Duhamel C, Lapinte V, Robin J. The use of renewable feedstock in UV-curable materials: a new age for polymers and green chemistry. Prog Polym Sci. 2013;38:932–62.
26. Wang Q, Chen G, Cui Y, Tian J, He M, Yang J. Castor oil based biothiol as a highly stable and self-initiated oligomer for photoinitiator-free UV coatings. ACS Sustain Chem Eng. 2016;5:376–81.
27. Ma L, Guo C, Ou R, Sun L, Wang Q, Li L. Preparation and characterization of modified porous wood flour/lauric-myristic acid eutectic mixture as a form-stable phase change material. Energy Fuel. 2018;32:5453–61.
28. Black M, Rawlins JW. Thiol–ene UV-curable coatings using vegetable oil macromonomers. Eur Polym J. 2009;45:1433–41.
29. Chen G, Guan X, Xu R, Tian J, He M, Shen W, Yang J. Synthesis and characterization of UV-curable castor oil-based polyfunctional polyurethane acrylate via photo-click chemistry and isocyanate polyurethane reaction. Prog Org Coat. 2016;93:11–6.
30. Ogunniyi DS. Castor oil: vital industrial raw material. Bioresour Technol. 2006;97:1086–91.
31. Liu Z, Fu X, Jiang L, Wu B, Wang J, Lei J. Solvent-free synthesis and properties of novel solid–solid phase change materials with biodegradable castor oil for thermal energy storage. Sol Energy Mater Sol C. 2016;147:177–84.
32. Kahwaji S, Johnson MB, Kheirabadi AC, Groulx D, White MA. Fatty acids and related phase change materials for reliable thermal energy storage at moderate temperatures. Sol Energy Mater Sol C. 2017;167:109–20.
33. Zeng J, Sun S, Zhou L, Chen Y, Shu L, Yu L, Zhu L, Song L, Cao Z, Sun L. Preparation, morphology and thermal properties of microencapsulated palmitic acid phase change material with polyaniline shells. J Therm Anal Calorim. 2017;129:1583–92.
34. Sarı A, Bicer A, Al-Ahmed A, Al-Sulaiman FA, Zahir MH, Mohamed SA. Silica fume/capric acid-palmitic acid composite phase change material doped with CNTs for thermal energy storage. Sol Energy Mater Sol C. 2018;179:353–61.
35. Del Barrio EP, Godin A, Duquesne M, Daranlot J, Jolly J, Alshaer W, Kouadio T, Sommier A. Characterization of different sugar alcohols as phase change materials for thermal energy storage applications. Sol Energy Mater Sol C. 2017;159:560–9.